Available online at www.sciencedirect.com

ScienceDirect

IFAC PapersOnline CONFERENCE PAPER ARCHIVE

IFAC PapersOnLine 53-2 (2020) 15053–15058

Measuring Urban Sidewalk Practicability: a Sidewalk Robot Feasibility Index

Matteo Corno * **Sergio Savaresi** *

* *Dipartimento di Elettronica Informazione e Bioingegneria, Politecnico di Milano, via G. Ponzio 34/5, 20133, Milan, Italy. Email: {matteo.corno, sergio.savaresi}@polimi.it. .*

Abstract: Autonomous parcel delivery is attracting a lot of interest. Terrestrial delivery drones travel at lower speeds, are smaller and lighter than passenger cars. These features make them an ideal and valuable first step and experimental sandbox toward fully autonomous vehicles. To be useful, however, small wheeled drones need to operate on parts of the roads that are reserved to pedestrians. This is a challenge by itself. Pedestrian areas are less structured than road and abide by looser rules. The best route for a delivery drone may not be the shortest path; other aspects need to be accounted for that make a route more or less practical for the specific features of the vehicle. This paper introduces a quantitative analysis of these specific issues. The paper proposes a quantitative index that asses a route practicability for a small terrestrial drone. It combines different aspects that account for sidewalk width, sidewalk surface condition, route length and the number of driveways and crosswalks present on the way. We provide the mathematical definition of the index, and use our wheeled drone prototype to show how it can be used to classify and chose the best routes among a selection. Although the index is designed for autonomous drones, given the specific dynamic features of the drone, it can also be employed as is to quantify the accessibility of different routes for disabled people.

Keywords: Robot navigation, Navigation system.

1. INTRODUCTION

In the past few years, autonomous driving has attracted a lot of attention, with self-driving cars and autonomous people movers as the main focus of attention. However, the change of purchasing habits has opened interesting opportunities for automated parcel delivery. It is estimated Joerss et al. (2016); Heutger et al. (2014) that more than half of the cost of a parcel delivery is due to the last mile and that more than 80% of the delivered parcels weigh less than a few kilograms. Moreover, delivery trucks and vans pose an issue in terms of traffic, pollution and efficiency. Amazon has been developing aerial delivery drones for some years air (2019). Aerial drones are problematic from the safety point of view. Terrestrial drones seem to be a more realistic solution in short-term. In particular, terrestrial drones small enough to navigate on the sidewalks and other traffic restricted areas are an interesting proposition Sabatini et al. (2018b,a).

In order to reach an elevated level of autonomy, a vehicle has to solve a number of tasks Choset et al. (2005):

(1) Global Path Planning. This task computes the best trajectory given the available information regarding starting and end point and maps.
(2) Sensing and Localization. The autonomous driving system needs to locate itself on the map and sense the presence of dynamic and static obstacles.
(3) Local Path Planning. The local path planner recomputes the path based on the actual environment. This replanning has to account for the traffic rules, position and velocity of other road occupants.
(4) Path tracking. This low-level controller controls the actuator to track the desired path.

Although this general framework is well accepted, different vehicles and application domains yield different level of complexity and call for different solutions. For example, in autonomous ships navigating open sea the localization problem is rather trivial (the GPS accuracy is often enough); the same problem is considerably more complex in urban navigation because of the tunneling effect and other GPS imprecisions.

In self-driving cars applications, the Global Path Planning problem is well discussed: many works focus on the definition of the best path in terms of time, traffic and fuel consumption Bast et al. (2016). The underlining assumption is that available map services provide detailed enough information for global path planning and that when a car-sized vehicle driving on roads is considered the most important factors are indeed time and efficiency. The issue changes when considering drones designed to operate in pedestrian zones. This types of drones behave differently from cars: they have different size, dynamic properties, sensing capabilities and operate in an environment that is less structured than roads with less clear traffic rules Trulls et al. (2011); Alahi et al. (2016); Capezio et al. (2011). For these reasons, one cannot use the classic methods to plan the *best* route.

10.1016/j.ifacol.2020.12.2025

This paper proposes a way to quantitatively assess different roads in a way that better accounts for the issues related to sidewalk navigation. In particular, we propose the Sidewalk Robot Feasibility Index (SRFI in the following) as a novel measure of how easy and safe it is for a robot to navigate a route. The SRFI is a collection of indexes intended to give a measure of quality of sidewalk routes taking into account four different factors that have a major impact on sidewalks navigability. The four factors are relative to the sidewalk width, the level of risk in pedestrian crossing, the number of driveways crossing the sidewalks and the quantity and entity of potholes and irregularities on the sidewalk surface. In the paper, we consider a drone prototype as a case of study, however it is interesting to note that the same index could be employed to assess how accessible a route is for disabled peoples.

The paper is structured as follows: In Section 2, we described the experimental setup. Section 3 defines the indexes composing the SRFI. Section 4 shows how the SRFI is applied to describe three possible routes connecting two point is Milan and considerations are made in order to choose the best one.

2. EXPERIMENTAL SETUP

The robot, called Yape, used in this work is depicted in Figure 1. It is a two wheeled self-balancing robot designed to perform autonomous parcel delivery in urban environments. Its two-wheeled architecture yields superior maneuverability, but makes the vehicle more sensitive to road asperities. Its sensing apparatus consists of a GPS, a 3D LiDAR and monocular cameras. The wheel motors

Fig. 1. Picture of the robot used in this work.

provide wheel rotational velocity and an inertial measuring unit mounted at the center of the wheelbase provides 3D accelerations and rotational rates.

3. SIDEWALK ROBOT FEASIBILITY INDEX DEFINITION

The objective of the SRFI index is to provide an objective description of the navigability of a certain route on urban sidewalks for Yape. The definition of the SRFI takes in part inspiration from the work published in Ferreira and da Penha Sanches (2007) where a sidewalk accessibility index for wheelchair users has been defined. The index is defined as a collection of sub-indexes each one describing the route according to a factor that is considered important for urban navigability:

$$SRFI = \begin{cases} I_{width} \\ I_{driveway} \\ I_{crosswalk} \\ I_{surf} \\ I_{length} \end{cases} \quad (1)$$

where:

- I_{width} that takes into account the width of the sidewalks
- $I_{driveway}$ takes into account the number of driveways with access to the sidewalk
- $I_{crosswalk}$ considers the number and the level of safety of pedestrian crossing that must be negotiated.
- I_{surf} takes into account the condition of the pavement on the route
- I_{length} considers the length of the route, simply defined as the length that the robot must travel to reach the destination.

Each sub-index is defined as a cost: considering a single sub-index, the higher the cost, the worse the route with respect to the relative criterion. Only routes that are considered to be feasible for the robot are described by the SRFI. The route is considered impracticable either if it presents a sidewalk with a width smaller than the robot or if at least one of the pedestrian crossings on the route presents sidewalks with no ramps. In the following each sub-index is described in detail.

3.1 Sidewalk Width

Considering a certain route, the sub-index related to the sidewalk width I_{width} is computed in two steps. First, the overall route is divided into sections where each section is defined as the longest consecutive portion of sidewalk that can be approximately considered of the same width. For each k-th section, l_k and w_k are defined as the length and the width of the sidewalk in that section and they are calculated using the measuring API of the Google Maps service. Figure 2 shows an example of how l_k and w_k are computed for two consecutive sections on a route. In a second step, each section is weighted

Fig. 2. Definition of the quantities of interest for the calculation of I_{width}.

depending on its width w_k using the penalizing function

of Figure 3. The function accounts for the width impact on Yape's navigation system. The worst possible case

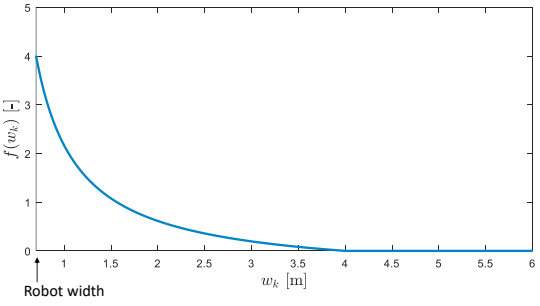

Fig. 3. Nonlinear penalizing function for the sidewalk width.

is a sidewalk with the same width of the robot (0.7 m in the case of Yape) while sections with a width greater than 4 meters have an associated cost of zero indicating an ideal situation. The nonlinearity of the function describes the fact that the difference between a 1-meter sidewalk and a 2-meter sidewalk has a larger impact on the navigation than the difference between a 3-meter and a 4-meter sidewalk. On a 2-meter sidewalk, the robot is able to circumnavigate a pedestrian without stopping; on sidewalks narrower than 1 meter, the robot is forced to stop and wait for the pedestrian to clear the way. The behavior on 3-meter or 4-meter sidewalks does not change.

Once each section has been penalized according to $f(w_k)$, the sidewalk index I_{width} is computed as a weighted summation of the cost attributed to each section:

$$I_{width} = \sum_{k=1}^{N} l_k f(w_k). \tag{2}$$

where N is the total number of section in the considered route. The cost of each section $f(w_k)$ is weighted in the overall index depending on how long the section is.

3.2 Driveways

In urban settings, driveways crossing the sidewalk to enable the access to buildings constitute a relevant factor of risk. Figure 4(a) shows one of the many driveways encountered in Milan. Figure 4(b) shows a frame recorded by Yape's on-board camera while navigating the sidewalk and approaching the driveway of Figure 4(a). Note the car backing up on the driveway: the driver has almost no visibility of the sidewalk and the driver relies on the sidewalk user to stop. The lack of visibility both from the robot side and from the car driver side makes this type of situation one of the most problematic while navigating. For this reason, the number of driveways crossing the sidewalk is taken into account in the SRFI formulation through the sub-index $I_{driveway}$. Considering a route, $I_{driveway}$ is simply defined as the number of driveways on the route n_{dw}. Driveways do not have any standard: one could claim that some driveways are more critical than others (in terms of visibility, width, etc.). Since it is difficult to objectively classify driveways depending on their risk level, they all are weighted equally in the sub-index $I_{driveway}$.

Fig. 4. Car traversing the sidewalk on one of the driveways encountered during the experiments.

3.3 Crosswalks

For a robot navigating on sidewalks, crossing a busy road is a critical action especially if there is not a traffic light ensuring a dedicated time slot to cross. Furthermore, street crossing slows down the robot navigation. These considerations are taken into account by $I_{crosswalk}$. It aims at penalizing both the quantity of street crossings and their risk level. $I_{crosswalk}$ is calculated in two steps. First, the possible types of crosswalks are classified in 5 categories and each category is weighted, from the easier to cross to the more difficult, using a weighting function similar to the one used for the sidewalk width. The five risk classes are:

(1) Crosswalks with dedicated pedestrians traffic light. The main road is characterized by a red traffic light while the pedestrian one is green, therefore vehicles need to stop even if there are no pedestrians.
(2) Crosswalks with dedicated pedestrians traffic light at intersections. Cars making a right turn can go through the crosswalk if there are no pedestrians waiting.
(3) Crosswalks without traffic light, zebra crossings are present.
(4) Crosswalks without traffic light at an intersection, zebra crossings are present.
(5) Crosswalks without zebra crossings.

Figure 5 shows an example of each risk class and their relative weight according to the nonlinear weighting function. The sub-index $I_{crosswalk}$ is numerically evaluated as:

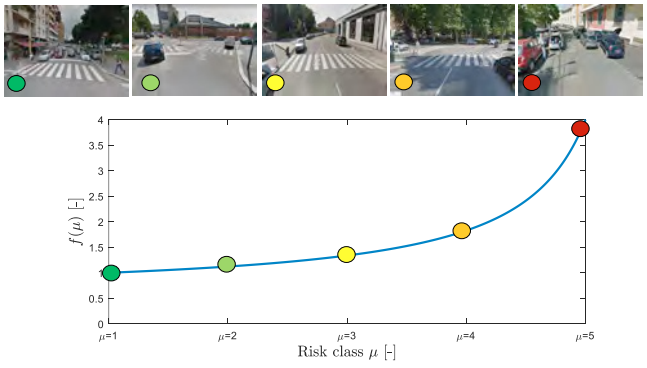

Fig. 5. Examples of crosswalks used during the experimental tests together with their impact on $I_{crosswalk}$ depending on their risk level.

$$I_{crosswalk} = \sum_{k=1}^{n_{cw}} f(\mu_k). \quad (3)$$

where n_{cw} is the number of crosswalks on the considered route.

3.4 Sidewalk Surface Condition

The fourth measure of sidewalk quality takes into account the condition of the sidewalk surface. Delivery robots are not intended to transport human being therefore comfort is not a priority when choosing a route. However, a sidewalk with big potholes and irregularities may be a problem for the integrity of the goods transported and, in some extreme cases, for the navigation itself. The sidewalk surface condition index I_{surf} is therefore intended to measure the quality of the sidewalk on a certain route in terms of number of surface irregularities and their level of unevenness. In order to make the index objective, the calculation of I_{surf} mainly relies on IMU measurements recorded while the considered route is navigated by the robot. The evaluation of the road irregularities is event based. A large vertical acceleration A_z triggers an event. Figure 6 summarizes the signal processing chain that detects these events. First, the vertical acceleration is high-

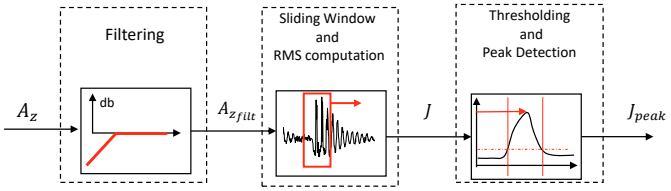

Fig. 6. Signal processing chain applied to the vertical accelerometer in order to detect sidewalk irregularities.

pass filtered in order to remove gravity and all the low frequency components related to the pitch dynamics of the robot. Then, an overlapping time sliding window of 1 second is considered and the root mean square of the filtered acceleration is computed in each window. The resulting signal J is used to detect road irregularities based on a threshold.

Figure 7(a) depicts Yape approaching an example of sidewalk irregularity where the ramp designed to get on the sidewalk is heavily damaged. Figure 7(b) shows the acceleration and speed recorded while Yape engages the ramp together with the resulting J signal. The road irregularity is clearly recognizable from the spike in J. Based on a threshold, the start and the end of the event are detected and the maximum over the length of the event is found (J_{peak}). J_{peak} alone is not a good representation of the irregularity; in fact its value depends on the road irregularity and the vehicle velocity. For this reason, J_{peak} is normalized. Figure 8 plots J_{peak} obtained by driving over a step at different speeds. The figure shows that, for the range of speed of interests, the speed influences J_{peak} in a linear way. Furthermore, the height of the step, that can be related to the level of unevenness of the sidewalk, changes the slope of this linear relationship. This result suggests the following normalization:

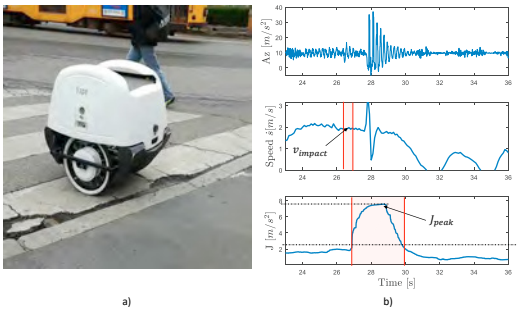

Fig. 7. On the left, Yape while facing a damaged ramp to get on the sidewalk. On the right, the signal of interest for the sidewalk irregularity detection while traveling on the ramp.

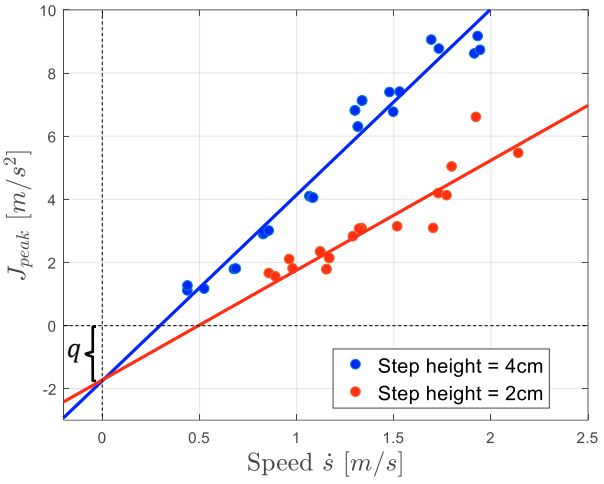

Fig. 8. Sensitivity of J_{peak} to the robot impact speed.

$$J_{peak_{norm}} = \frac{J_{peak} - q}{v_{impact}} \quad (4)$$

where q is the intercept of the lines plotted in Figure 8. Defined in this way, $J_{peak_{norm}}$ is a proxy of the level of roughness of the sidewalk in that point.

Like for the other indexes, $J_{peak_{norm}}$ is weighted in a nonlinear way in order to heavily penalize the most critical events. Figure 9 shows some examples of sidewalk irregularities together with the related penalization values and the measured vertical accelerations.

I_{surf}, that measures the quality of the sidewalk surface on the overall route, is defined similarly to $I_{crosswalk}$ in (3):

$$I_{surf} = \sum_{k=1}^{n_{surf}} f(J_{peak_{norm_k}}) \quad (5)$$

where n_{surf} is the number of irregularities detected on the selected route. Note that this is the only index, among the ones employed, that requires ad-hoc measurements and that cannot be reconstructed by other sources. This is however compatible with Yape level of autonomy, Yape is in fact designed to autonomously navigate roads that have been previously mapped and analyzed while being remotely guided.

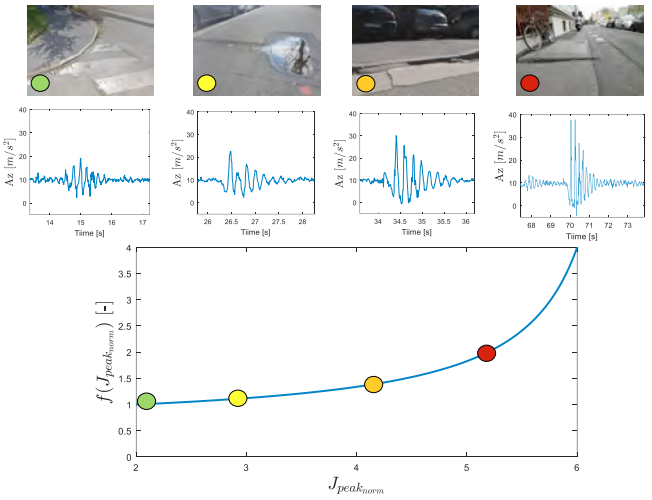

Fig. 9. Examples of sidewalk irregularities together with their impact on I_{surf} according to relative penalizing function.

4. ROUTE COMPARISONS

In order to better illustrate the qualities of the proposed method. The SRFI indexes are computed for each of the three routes displayed in Figure 10. Route 1 is the shortest

Fig. 10. Three possible routes connecting starting and end location of the considered delivery use-case.

and the one suggested for pedestrians by the Google maps service. The other two routes are slightly longer alternatives. The results are presented in Figure 11 where the four plots on the top represent the raw values of the indexes while the plot on the bottom represents the same indexes, with the addition of the route length, normalized by the score obtained by the best route in each category.

Two spikes are evident looking at the normalized values: the high score in sidewalk width for route 1 and the high score in sidewalk surface condition in route 2. This clear indication is in line with the impressions that the author had driving the robot through the routes. Regarding the surface condition, while remote controlling Yape along route 2, significantly more critical road irregularities have been encountered compared to the other two routes, some of them are indicated on the map in Figure 12. Regarding the sidewalk width, Figure 12 illustrate some examples on the map for each of the three routes: it is easy to notice how route 1 presents much smaller sidewalks compared to

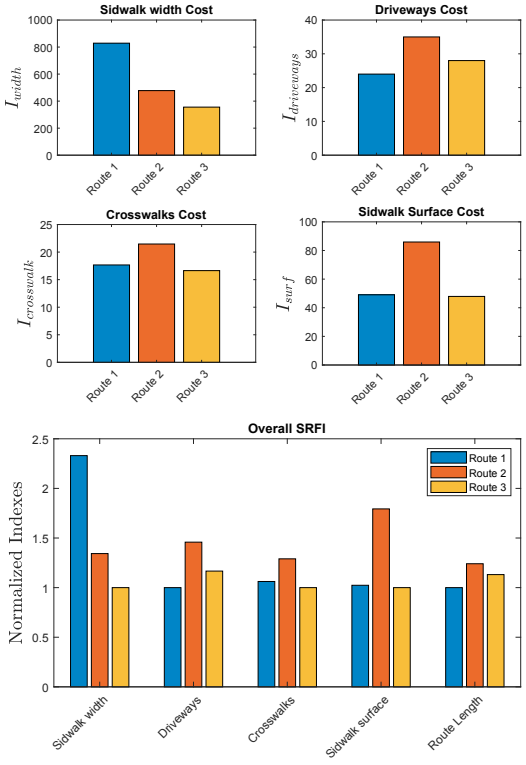

Fig. 11. Comparison of the three considered route based on the SRFI calculation.

route 3. In particular, during the experiment, route 1 was judged very challenging to navigate due to the very small sidewalk pictured in Figure 12.

Since the SRFI is a collection of different evaluation criteria, choosing the best route means solving a multi-objective optimization problem. It is not straightforward to find a solution that is optimal overall since, most of the times, the various costs function are in conflict with each other. Therefore, in this kind of problems, the objective becomes to find a set of efficient or non-dominated solutions called Pareto front. Looking at the cost functions of the set of three route presented in Figure 11, it is clear that route 2 does not belong on a Pareto front because it is entirely dominated by route 3, hence it should be discarded from the decision process. Route 3 and 1 are not dominating each other and a decision among them can only be made expressing a ranking of importance between the multiple criteria. Yape's localization and planning features suggest to give more weight to the width of the sidewalks. In conclusion, route 3 is considered the best of the three.

5. CONCLUSIONS

This paper presents the SRFI as a measure of route practicability on urban sidewalks. It has been defined as a collection of indexes taking into account sidewalk width, sidewalk surface condition, route length and the number of driveways and crosswalks present on the way. The index has been used to evaluate the best route among three possible routes. The SRFI highlights some issues with the

Fig. 12. Maps of the three considered route where the sidewalk width is highlighted using a color code. Some critical situations are displayed for route 1 and 2.

shortest route suggested by Google maps and redirects the choice of the best route to route number 3.

The SRFI index here presented can be used to run state of the art routing algorithms on the whole urban network. In particular, since it consists of a collection of sub-indexes, the SRFI is well suited to be used with algorithm solving the Multi Objective Shortest Path Problem (MSPP) that is a special case of a multi-optimization problem (see Pangilinan and JANSSENS (2007)). Since, in most cases, a single optimal path does not exist, a routing algorithm could use the SRFI index to find a set of efficient solutions belonging to the Pareto front.

6. ACKNOWLEDGMENT

Financial support by Yape s.r.l. is acknowledged.

REFERENCES

(2019). Amazon official website. https://www.aboutamazon.it/innovazioni/prime-air, 2019.

Alahi, A., Goel, K., Ramanathan, V., Robicquet, A., Fei-Fei, L., and Savarese, S. (2016). Social lstm: Human trajectory prediction in crowded spaces. In *Proceedings of the IEEE Conference on Computer Vision and Pattern Recognition*, 961–971.

Bast, H., Delling, D., Goldberg, A., Müller-Hannemann, M., Pajor, T., Sanders, P., Wagner, D., and Werneck, R.F. (2016). Route planning in transportation networks. In *Algorithm engineering*, 19–80. Springer.

Capezio, F., Mastrogiovanni, F., Scalmato, A., Sgorbissa, A., Vernazza, P., Vernazza, T., and Zaccaria, R. (2011). Mobile robots in hospital environments: an installation case study. In *ECMR*, 61–68.

Choset, H.M., Hutchinson, S., Lynch, K.M., Kantor, G., Burgard, W., Kavraki, L.E., and Thrun, S. (2005). *Principles of robot motion: theory, algorithms, and implementation*. MIT press.

Ferreira, M.A. and da Penha Sanches, S. (2007). Proposal of a sidewalk accessibility index. *Journal of Urban and Environmental Engineering*, 1(1), 1–9.

Heutger, M., Kückelhaus, M., Zeiler, K., Niezgoda, D., and Chung, G. (2014). Self-driving vehicles in logistics.

Joerss, M., Schröder, J., Neuhaus, F., Klink, C., and Mann, F. (2016). Parcel delivery: The future of last mile. *McKinsey & Company*.

Pangilinan, J.M.A. and JANSSENS, G. (2007). Evolutionary algorithms for the multi-objective shortest path problem.

Sabatini, S., Corno, M., Fiorenti, S., and Savaresi, S.M. (2018a). Improving occupancy grid mapping via dithering for a mobile robot equipped with solid-state lidar sensors. In *2018 IEEE Conference on Control Technology and Applications (CCTA)*, 1145–1150. IEEE.

Sabatini, S., Corno, M., Fiorenti, S., and Savaresi, S.M. (2018b). Vision-based pole-like obstacle detection and localization for urban mobile robots. In *2018 IEEE Intelligent Vehicles Symposium (IV)*, 1209–1214. IEEE.

Trulls, E., Corominas Murtra, A., Pérez-Ibarz, J., Ferrer, G., Vasquez, D., Mirats-Tur, J.M., and Sanfeliu, A. (2011). Autonomous navigation for mobile service robots in urban pedestrian environments. *Journal of Field Robotics*, 28(3), 329–354.